ChemPlusChem

Research Article
doi.org/10.1002/cplu.202300502

Chemistry Europe
European Chemical Societies Publishing

www.chempluschem.org

Special Collection

Puzzling Structure of the Key Intermediates in Gold(I)-catalyzed Cyclization Reactions of Enynes and Allenenes

Eduardo García-Padilla,[a, b] Imma Escofet,[a, b] Feliu Maseras,[a, b] and Antonio M. Echavarren*[a, b]

We identify the dominant structures of the intermediates of gold(I)-catalyzed cyclizations of 1,5-enynes and 1,5-allenenes through computational analysis as gold(I) cyclopropylcarbenes, endocyclic vinylgold complexes and previously unreported non-classical carbocationic minima. In contrast to 1,6-enynes, the exocyclic carbocations are found to be less stable. Cyclopropylcarbene structures are consistently favoured as the most stable intermediates for all studied substitution patterns. We validate the computational methods used by using DLPNO-CCSD(T) energies as a benchmark, indicating that the B3LYP-D3 and M06-D3 functionals are most accurate for energy determination, while NPA charges are mostly insensitive to functional. The evolution of a 1,6-enyne in a single-cleavage or double-cleavage rearrangement is attributed to the barrierless evolution of a common cyclopropyl–gold(I) carbocation non-stationary geometry. Our findings provide insights into reaction pathways and substrate dependence of the cycloisomerization processes.

Introduction

Gold(I) carbenes have been proposed as intermediates of many gold(I)-catalyzed transformations, although there is still some controversy regarding the carbenic and cationic character of these species.[1,2] Although they are too highly reactive to be readily isolated, some progress has been done in the characterization of these species albeit stabilizing functional groups attached to the carbenic carbon were required.[3] Indeed, our group has recently generated mesityl gold(I) carbenes in solution at very low temperature, which have been characterized by NMR.[4]

As part of an in-depth mechanistic study on a gold(I)-catalyzed cyclization leading to *cis*- or *trans*-fused bicyclo-[5.1.0]octanes,[5] we examined the nature of the key intermediates, which was relevant in the broader context of the gold(I)-catalyzed cyclization of 1,6-enynes.[2,6,7] This computational study provided evidence on the existence of three different types of cationic intermediates **Int2**–**4** depending on the substituents R^1-R^4 in the initial gold(I) complex **Int1** (Scheme 1). Benchmark of DFT functionals with DLPNO-CCSD(T) as calibration method,[8] allowed us to select the most appropriated functional for the 1,6-enynes cyclizations. Cyclopropyl gold(I) carbene **Int2**, exocyclic vinylgold carbocation **Int3**, and endocyclic vinylgold carbocation **Int4** were located as possible minima having different bond angles and distances. The quantum theory of atoms in molecules (QTAIM)[9] analysis supported the molecular representation of the different types of intermediates. The metal carbenic or cationic character of these intermediates **Int2**, **Int3** and **Int4** was further confirmed by Natural Bond Orbital (NBO) analysis,[10] as natural population analysis (NPA) charges were clearly delocalized. In the model substrates where cyclopropyl gold(I) carbene **Int2** and open carbocation **Int3** were found as possible intermediates, the former was always preferred kinetically ($\triangle G^{\ddagger}$ for **TS1**–**2** lower than for **TS1**–**3**) and thermodynamically. In those cases, **Int4** was not found alongside **Int2** and **Int3**.

In a recent study on the anomalous gold(I)-catalyzed *Z*-selective skeletal rearrangement of 1,6-enynes we have found that the electronic nature of the substituents at the alkene determine the stereoselectivity in single-cleavage rearrangements.[11] Thus, open form exocyclic carbocations **Int3** are favored when R^2 is a strongly electron-donating group and can undergo bond rotation, whereas cyclopropyl gold(I) carbenes **Int2** do not isomerize and lead to rearrangement products stereospecifically.

Due to the fundamental importance of cyclizations of unsaturated substrates in gold(I) catalysis, we present herein a detailed computational study on the structures of the key intermediates in the cyclization of seemingly similar 1,5-enynes and 1,5-allenenes, including a complete NBO study aiming to rationalize the relative stabilities of each structure and their dependence on different substitution patterns. For the sake of

[a] E. García-Padilla, Dr. I. Escofet, Prof. F. Maseras, Prof. A. M. Echavarren
Institute of Chemical Research of Catalonia (ICIQ-CERCA)
The Barcelona Institute of Science and Technology (BIST)
Av. Països Catalans 16
43007 Tarragona (Spain)
E-mail: aechavarren@iciq.es

[b] E. García-Padilla, Dr. I. Escofet, Prof. F. Maseras, Prof. A. M. Echavarren
Departament de Química Analítica i Química Orgànica Universitat Rovira i Virgili (URV)
C/ Marcel·lí Domingo s/n
43007 Tarragona (Spain)

Supporting information for this article is available on the WWW under https://doi.org/10.1002/cplu.202300502

Special Collection Part of a Special Collection on Gold Chemistry

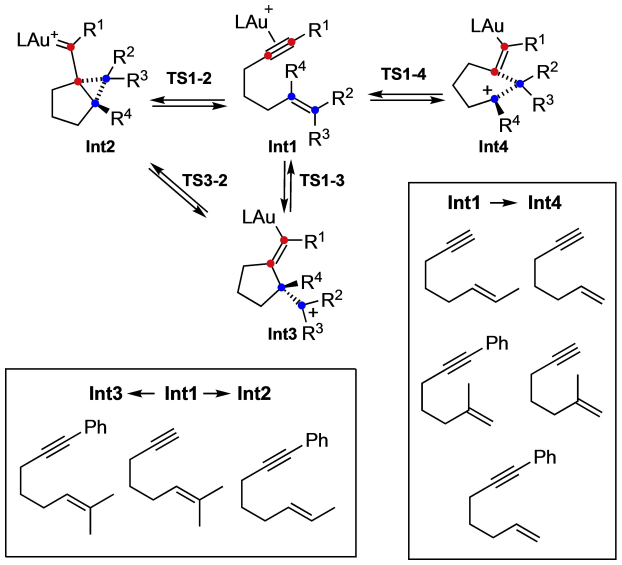

Scheme 1. Different possible pathways for the formation of **Int2**, **Int3** and **Int4**. L = PMe_3.

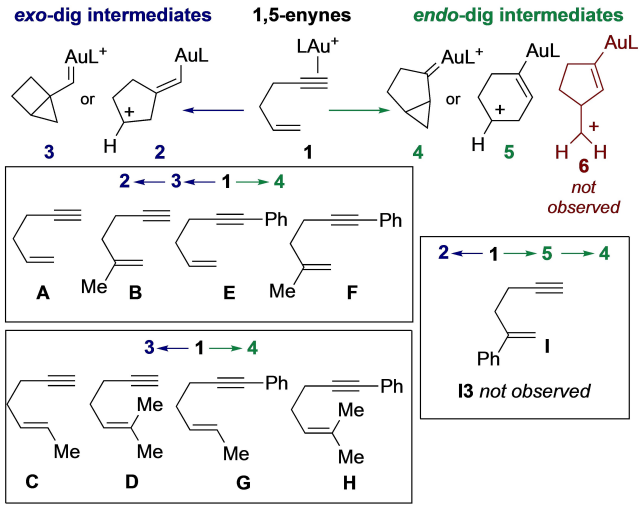

Scheme 2. 1,5-enynes **A**–**H** with the same substitution patterns as the previously studied 1,6-enynes were calculated as the gold(I) complex (**A1**–**I1**), the *exo* (**A2**–**I2** and **A3**–**I3**), and *endo* (**A4**–**I4**, **A5**–**I5**, and **A6**–**I6**) intermediates. L = PMe_3.

completeness, we have also analyzed the subtle differences leading to either single- or double-cleavage rearrangements in gold(I)-catalyzed reactions of 1,6-enynes.

Results and Discussion

Nature of intermediates in 1,5-enyne cyclizations. We aimed to investigate intermediates present in the 5-*endo*-dig, 5-*exo*-dig, and 4-*exo*-dig cyclizations of 1,5-enynes. The 4-*exo*-dig cyclizations are typically less favorable due to strain and orbital overlap, as explained by Baldwin's rules. Including these less favorable intermediates and transition states in our study served three primary purposes: first, to directly compare with the established 1,6-enyne *exo*-dig analogues (Scheme 1), but with added ring strain; second, to reproduce the observed experimental preference for the alternative pathway; and third, to understand how strain influences the bonding or even prevents certain geometries. To approach this problem, we carried out DFT calculations on a set of gold(I) complexes of 1,5-enynes. Full computational details are supplied in the Supporting Information, and all computed structures are collected in the ioChem-BD repository.[12] The geometry optimizations and free energy analysis reported in this first part were carried out with BP86-D3, a functional consisting of Becke's exchange functional and Perdew's 1986 correlation functional,[13] with implicit solvation modelled with PCM for CH_2Cl_2. This, in turn, will allow direct comparison to our aforementioned published results on 1,6-enynes (Scheme 1).[5]

A series of model 1,5-enynes **A**–**H** were chosen to include varied alkyl substitution on the alkene, with a terminal or phenyl-substituted alkyne (Scheme 2). The methyl groups on the alkene could, in principle, alter the electronics of the system to favor some structures of cyclized intermediates, as had been observed with 1,6-enynes.[5] The phenyl-substituted alkynes were included because internal alkynes with aryl substituents have been extensively studied experimentally. Substrate **I** was also included with a strongly electron-donating substituent at C2 of the alkene to see if a 4-*exo*-dig cyclisation still has an accessible reaction coordinate, or whether it would collapse to the same reaction coordinate as the 5-*exo*-dig cyclization.

For the methyl-substituted 1,5-enynes, geometries **5** and **6** for the first cyclized intermediates were always inaccessible, converging in a barrierless manner into cyclopropyl gold(I) carbene **4** (Scheme 2 and Table 1). In addition, **C2**, **D2**, **G2**, and **H2** geometries did not constitute minima on the potential energy surface and were not considered for the analysis as they did not represent the intermediates of interest in gold(I) catalysis. A phenyl substituent next to the formed carbocation stabilize it enough for the open form to exist as an independent intermediate as seen in **I5**. 1,5-Enyne **I** was only explored to increase the stability of the open form carbocation, explaining the absence of a bicyclopentane geometry. Despite this significant benzylic stabilization, it is remarkable how intermediate **I5** has still somewhat higher energy than cyclopropyl gold(I) carbene **I4**. The formation of a bicyclic structure with relatively low strain combined with a stabilized gold(I) carbene contributes to the overall stability of the intermediate (Table 1).[14]

After having the relative energies of all intermediates accessible for every 1,5-enyne and discarding several of the structures as inaccessible, we investigated the possible bonding arrangements for these intermediates. An NBO analysis of selected intermediates was carried out. **H3**, **H4**, **B2**, **B3**, and **I5** were chosen, representing the endocyclic cyclopropyl gold(I) carbene, a strained exocyclic cyclopropyl gold(I) carbene, an endocyclic carbocationic vinyl gold(I) complex, its strained cyclopropylcarbene analogue, and an endocyclic carbocationic cyclohexenylgold complex (Scheme 3).

The NPA charges (from NBO) show a similar charge distribution for **H3** and **H4** independent from the ring size. The

Table 1. Calculated free energies in kcal/mol, referenced to **1** at B3LYP-D3/6-311+G(d,p) [C,H,P]+SDD [Au], with implicit solvation (PCM). In cases where free energy is lower for the TS, the potential energy thereof was confirmed to be higher.

Enyne	Species	ΔG‡	ΔG°
A	**A2**	20.9[a]	19.1
	A3	21.7	17.5
	A4	13.0	−1.9
B	**B2**	12.2[a]	9.1
	B3	17.3	12.4
	B4	10.6	−1.7
C	**C3**	19.1	17.8
	C4	11.5	−1.5
D	**D3**	16.0	18.7
	D4	10.1	0.0
E	**E2**	25.6[a]	23.9
	E3	25.4	20.4
	E4	15.2	3.5
F	**F2**	12.6[a]	10.7
	F3	18.9	13.9
	F4	9.0	0.5
G	**G3**	23.4	20.9
	G4	15.3	2.7
H	**H3**	11.2	4.3
	H4	21.8	23.1
I	**I2**	18.7	4.2
	I4	2.4[b]	1.2
	I5	12.8	2.6

[a] TS corresponds to $\mathbf{TS_{2-3}}$. [b] TS corresponds to $\mathbf{TS_{4-5}}$.

differences between **H3** and **B3** are much more significant, exemplifying how the charge localization on the original alkene carbons depends on their substitution more than on their specific bonding arrangement. **B2** and **I5** show comparable charge distributions.

In order to investigate the bonding of these intermediates, with the aim of describing their cyclopropylcarbene or open form carbocationic character, we decided to study them through second-order perturbation theory, which explains the non-Lewis character of molecules through delocalization of the occupied NBOs (Lewis structure-based orbitals) into the unoccupied NBOs.

Performing the same calculations on known 1,6-enyne intermediates **Int2**, **Int3**, and **Int4** (Schemes 1 and 3), with special emphasis on the second-order perturbation theory, allowed the direct quantitative comparison to the explored intermediates of 1,5-enyne cyclizations (Scheme 3). Thus, **Int2** shows a lower occupancy of the endocyclic cyclopropyl bond compared to the exocyclic (1.639 and 1.750 respectively). This correlates with the results from second-order perturbation theory, as the donation from C–C_{endo} bond to the gold carbene is, at 23.6 kcal/mol, three times higher than that from C–C_{exo}. Similarly to **H3**, **H4** and **B3**, as a rule, it is the *endo*-bond of the cyclopropyl the one that delocalizes best for electronically unbiased cyclopropyl gold(I) carbenes. In line with being an open-form intermediate, **Int3** only shows a very small delocalization of the alkene onto the carbocation, whereas the hyperconjugation from the adjacent C–C is almost twice as strong. We also observed this in **I5**, which corresponds to a true carbocationic form. The inner cyclopropyl bond for **Int4** is much less populated than the exocyclic one, by 0.3 electrons. This is compounded by more delocalization from the inner bond to the carbene (35.3 kcal/mol) and a donation that is nine times lower from the exocyclic bond. Combined, these observations indicate that **Int4** lies somewhere between a closed cyclopropylcarbene and an open form. We consider that this intermediate is probably best described as a highly polarized version of **Int2** rather than as a separate geometric category.

Compared to **B3**, **B2** is more polarized. However, by looking at the second order perturbation theory analysis, even open-form **B2** shows very significant donation from C–C π to carbocation (**B2a** resonance structure) as well as strong C–C σ donation to carbocation (**B2b** resonance structure) (Scheme 4). These donations, 89 and 72 kcal/mol respectively, are very significant. Both are much stronger than the expected C–H hyperconjugation (15 kcal/mol). This strong donation from both the double bond and the adjacent single bond suggests that even the open form **B2** has significant cyclopropyl character. This is likely enhanced by the constrained geometry of a small

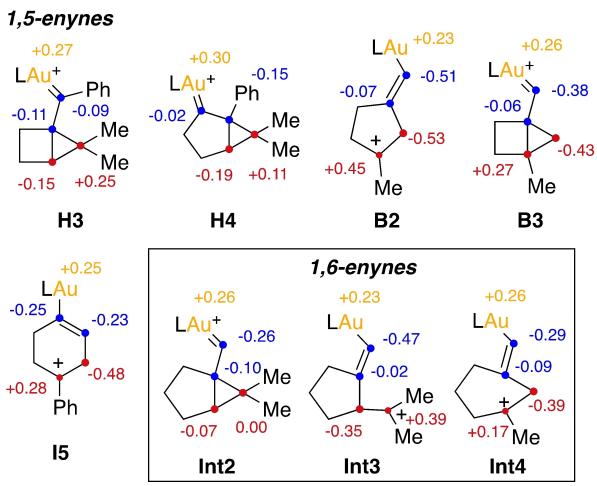

Scheme 3. NBO charges from NPA of 1,5-enynes, 1,6-enynes. L = PMe_3.

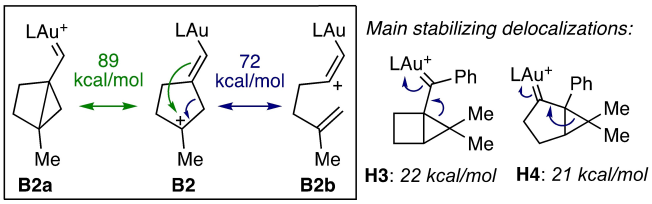

Scheme 4. NBO delocalizations stabilizing intermediate **B2**, depicted as resonant forms and energy of delocalization from the outer cyclopropylic bond NBO.

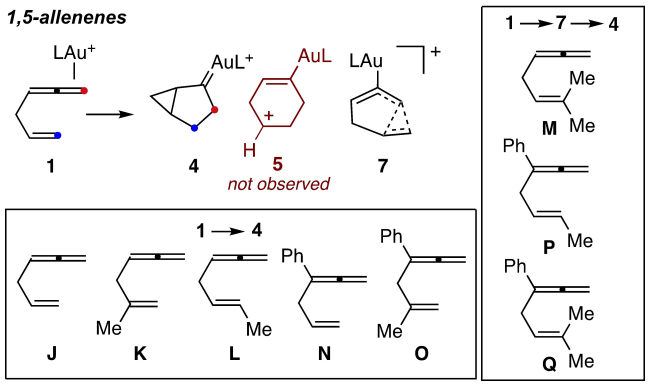

Scheme 5. 1,5-allenenes **J**–**Q** with the same substitution patterns were calculated as the gold(I) complex (**J1**–**Q1**) and as (**J4**–**Q4** and **J7**–**Q7**) intermediates. L = PMe_3.

cycle allowing for better orbital overlap. In contrast, in **I5** instead of the vinylgold to carbocation donation, the more significant stabilizing interaction is the hyperconjugative σ C–C to carbocation donation (21.3 kcal/mol). As expected, there is an additional benzylic stabilization. Intermediate **I5** is therefore a true open form vinylgold(I) carbocation (Scheme 3).

Comparing intermediates **H3** and **H4** by NBO analysis shows differences in the cyclopropyl rings (Scheme 4). In both cases, it is the outer cyclopropyl bond which has the lowest occupancy, just under 1.7 in both cases. This is likely a result of the potential stabilization offered by the methyl groups. The main difference is in the occupancy of the inner cyclopropyl bond, at 1.825 for **H4** but at 1.754 for **H3**. The donation from either of the outer cyclopropyl bonds to the gold(I) carbene is surprisingly similar, between 20 and 22 kcal/mol, despite the gold(I) carbene being endocyclic or exocyclic. Backdonation from the carbene is nonetheless significant in the case of **H3**.

Nature of intermediates in 1,5-allenene cyclizations. We then explored a related family of substrates, 1,5-allenenes **J**–**Q** (Scheme 5). These compounds with two geminal π bonds cannot lead to the synchronous formation of cyclopropyl gold(I) carbenes, given that this geometry necessitates a triple bond. It is for this reason that reported reactions with allenenes often invoke open-form carbocationic vinylgold(I) intermediates as opposed to the more delocalized cyclopropyl gold(I) carbenes.[15] Nonetheless, the tether in 1,5-allenenes is short enough for a cyclopropyl to form with the second alkene.[16] As the cyclopropanation occurs from the other side, the bond to be formed in the cyclization is not part of the cyclopropane. This is interesting, as both 1,5-allenenes and 1,5-enynes lead to the same carbon skeleton, but this is formed in a different way. Reactions with 1,6-allenenes have been found to operate analogously via cyclobutyl gold(I) carbene intermediates instead.[17]

All currently proposed mechanisms with 1,5-allenenes suggest the presence of an endocyclic carbocation within a cyclohexenyl gold(I) structure **5** (Scheme 5). However, we have already determined that, in all instances involving 1,5-enynes, these configurations are non-stationary geometries except when an aryl group stabilizes the carbocation. This brought us to question whether these geometries could be intermediates for 1,5-allenenes, possibly due to divergent formation through a high-energy intermediate, or if they also exist only as non-stationary points in the concerted asynchronous formation of bicyclo[3.1.0]hexanes. In non-stepwise processes, the intermediacy of generally disfavored endocyclic carbocations could be expected as well-defined non-stationary points with barrierless evolution in the reaction coordinate, also known as hidden intermediates.[18] These hidden intermediates, while being relatively widespread in asynchronous processes, rarely determine the outcome of a reaction. However, they have been found in rearrangements of unsaturated systems and were key to understanding the selectivity in the reaction.[19b] In order to make direct comparisons to the 1,5-enyne cyclizations, we studied a family of 1,5-allenenes with the same substitution patterns on the alkene. Similar to the analogous 1,5-enynes **A**–**H**, it was observed that endocyclic homoallylic cations exhibit non-stationary geometries in the potential energy surface (Scheme 5). Consequently, and at least for the substrates under investigation, the intermediate that follows cyclization is the cyclopropyl gold(I) carbene **4**. A feature of 1,5-allenenes not present for 1,5-enynes is that, upon cyclization, non-classical carbocations **7** can exist as intermediates. These structures correspond to partial cyclopropyl carbenes, due to the absence of the second π bond that would lead to a conventional cyclopropylcarbene (Scheme 5 and Table 2).[11]

Whereas most other intermediates are formed in concerted asynchronous processes, the formation of **P7**, **M7**, and **Q7** takes place stepwise. The most delocalized form, with both cyclopropyl bonds approximately equal, is present in intermediate **P7**. On the other hand, intermediates **M7** and **Q7** resemble more open-form carbocationic structures, in which dimethyl-substituted alkenes favor the localization of charge on the tertiary carbocation (Scheme 6). The endocyclic alkene cannot stabilize the exocyclic carbocation because of the geometry, which results in the exocyclic vinylgold(I) carbocation intermediate, a type of intermediate that was never observed for the 1,5-enynes. A corollary is that cyclizations of 1,5-allenenes with

Table 2. Calculated free energies in kcal/mol, referenced to **1** at B3LYP-D3/6-311 + G(d,p) [C,H,P] + SDD [Au], with implicit solvation (PCM).

Allenene	Species	$\Delta G^{\ddagger}$	ΔG°
J	**J4**	14.1	0.6
K	**K4**	9.0	-0.5
L	**L4**	11.8	2.5
M	**M4**	17.3[a]	3.8
	M7	8.9	8.3
N	**N4**	13.6	1.5
O	**O4**	7.7	0.0
P	**P4**	13.8	3.6
	P7	11.8	11.0
Q	**Q4**	7.8	4.3
	Q7	16.3[a]	6.8

[a] TS corresponds to **TS4**–**7**.

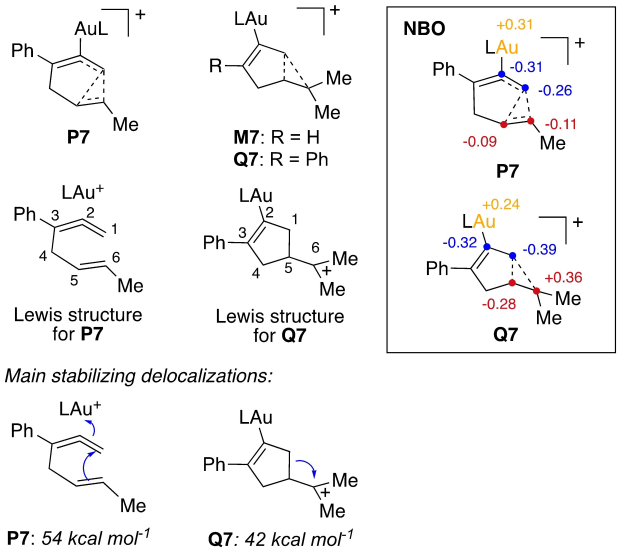

Scheme 6. Structures of intermediates **P7**, **M7** and **Q7** and NBO analysis from NPA of **P7** and **Q7**. L = PMe_3.

gold(I) catalysts show more carbocation-like reactivity than with 1,5-enynes.

The nature of the bonds in these intermediates was explored with NBO analysis by using **P7** and **Q7** as the model systems. As would be expected from a more open-form geometry, there was a much higher charge localization in **Q7** (Scheme 6).

The NBO analysis fully supports a non-classical carbocation description for **P7** (Scheme 6). The base Lewis structure without cyclopropyl bonds showed very low occupancies for alkenes C1–C2 and C5–C6, around 1.6, with partially populated anti-bound, at occupancies of 0.1. Donation of π C5–C6 to π* C1–C2 accounted for a very large stabilization of 54 kcal/mol according to second-order perturbation theory. These contributions, together with the low occupancy, are indicative of strongly delocalized π bonds reminiscent of aromatic bonds. The non-classical carbocationic structure is therefore a proper representation of this intermediate.

Intermediate **Q7** is much more localized and better described by its Lewis structure. However, the C1–C5 bond has an occupancy of 1.785 and the carbocation, notably, 0.608. The delocalization of the former onto the carbocation is the greatest contributor to its stabilization, at 42 kcal/mol, consistent with partial cyclopropyl character, but no more than in most open-form intermediates studied hitherto (Scheme 6). Structure **Q7** is more localized than endocyclic vinylgold(I) carbocation **B2**, again, because the bond delocalizing into it is a σ bond instead of the inaccessible alkene.

Benchmark of DFT functionals. An additional question concerned the suitability of different functionals to correctly represent the bonding in these systems. To address this, we performed a series of single-point calculations of many intermediates using different families of functionals, with implicit solvation and applying Grimme's D3 empirical dispersion.[20] To quantify the relative performance of each functional, we carried out analogous DLPNO-CCSD(T) single-point calculations with ORCA 4.0 to serve as a benchmark. This approach was already used with 1,6-enynes in our previous work,[5] which concluded that B3LYP–D3 and M06-D3 were the most appropriate functionals. The intermediates with substrate **I** were calculated to ensure that carbocationic species are described in a similar way. One of the main aspects of interest was whether different functionals would accurately depict low-lying transition state **TSI4–5**, which was very close in energy to **I5**, making this system a challenging model.[21] The benchmark was repeated with cyclized **H** species.

Hence, there is a preference for B3LYP–D3 or M06-D3 to be used as the functionals in the determination of the final energy profiles. Nevertheless, further calculations suggested that the geometry optimization of the studied gold(I) intermediates is likely not sensitive to the functional used.[21]

Further insight on the skeletal rearrangement of 1,6-enynes. Two main types of skeletal rearrangements of 1,6-enynes are known: single-cleavage, in which only the alkene suffers a metathesis-type cleavage and the double-cleavage rearrangement in which both the alkyne and alkene undergoes metathesis (Scheme 7).[2a,7,22] These main types have also been known as type I and type II rearrangements. Furthermore, two subtypes of single-cleavage rearrangement, *exo*- and *endo*-type, can occur which essentially depend on the nature of the tether Z.[11,23] The *endo*-type single-cleavage has also been referred to in the literature as type III rearrangement. The gold(I)-catalyzed double-cleavage rearrangement of 1,6-enynes is the preferred cycloisomerization process for substrates bearing internal alkynes and terminally unsubstituted alkenes. Experimentally, there have been some observations made on the effect that different substituents have on the single/double cleavage selectivity,[24] whereas theoretical studies have been reported on Pt(II)-, Au(I)-,[25] and In(III)-catalyzed rearrangements.[26]

We decided to investigate in detail a simplified model substrate to understand why double-cleavage rearrangements happen and why mixtures of single- and double-cleavage products are rarely reported from the same substrate.

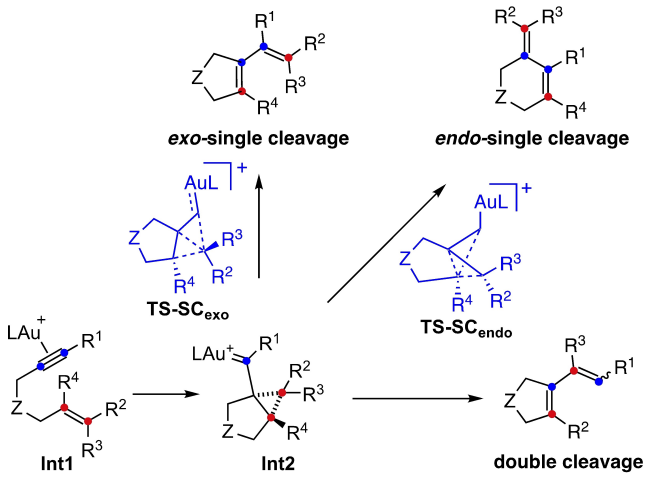

Scheme 7. Different skeletal rearrangement pathways from 1,6-enynes.

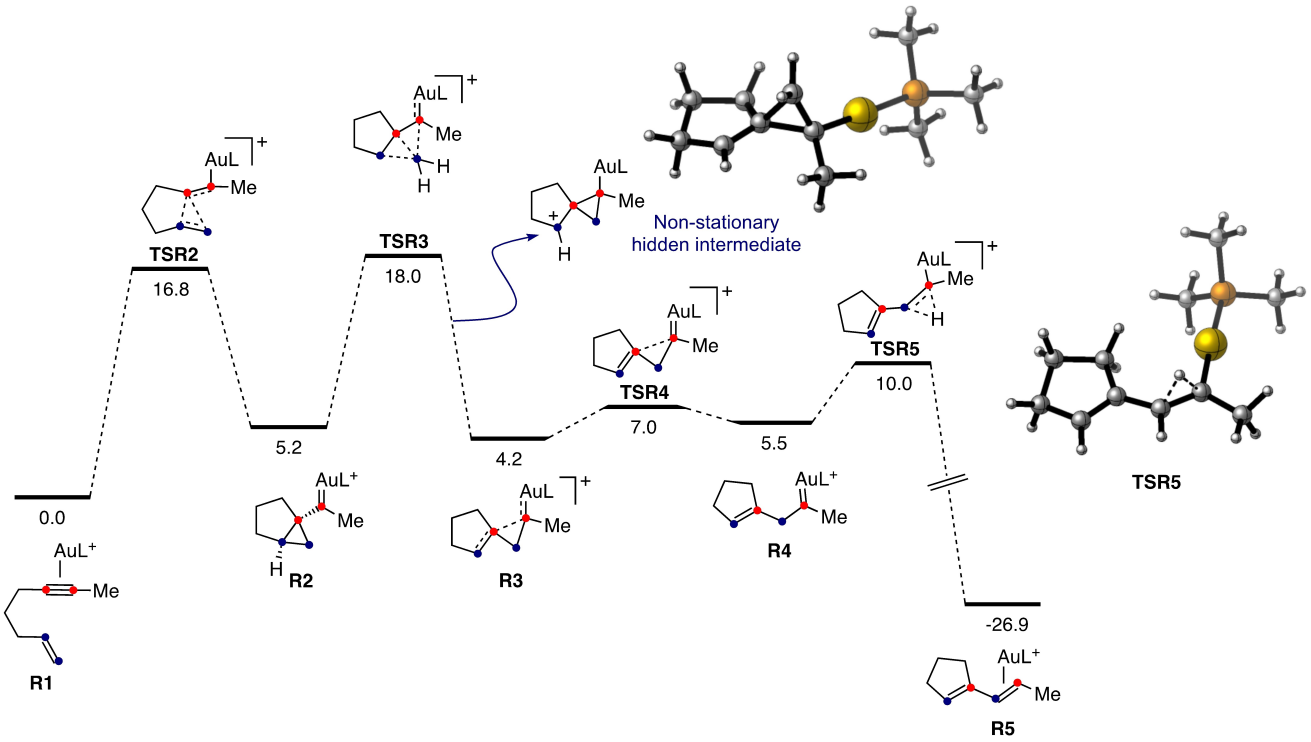

Scheme 8. Mechanism of the double-cleavage rearrangement of a model 1,6-enyne. L = PMe_3. Free energies in kcal/mol calculated at B3LYP–D3/6-311 + G(d,p) [C,H,P] + SDD [Au], PCM (dichloromethane).

1-Octen-6-yne, as the simplest model enyne, was chosen for the mechanistic modelling as our previous results[11] suggested that the impact of the tether only affects *exo*- and *endo*-type cleavage selectivity, which is not present in double cleavage reactions. The gold(I) complex **R1** undergoes a 5-*exo*-dig cyclization leading to cyclopropyl gold(I) carbene **R2** (Scheme 8). The following rate-limiting migration **TSR3** is analogous to that in the exocyclic single cleavage process.[11]

As observed in the IRC, **TSR3** lies at the highest potential energy of a two-step concerted asynchronous process which proceeds through a non-stationary geometry or hidden intermediate[18] when relaxing to the product (Figure 1 and Scheme 8, shown in blue). This structure is reminiscent of cyclopropylgold(I) carbocations in the endocyclic single-cleavage mechanism (Figure 2). However, in this case, the structure is not a minimum and relaxes to **R3** without a potential energy barrier.

The C_{alkene}–C–Au bond angle in **R3** is 90.1°, indicative of a strong delocalization from the alkene to the gold(I) carbene, not unlike the intermediates discussed previously for 1,5-enynes and 1,5-allenenes. A shallow transition state, **TSR4**, leads to open form **R4** without alkene stabilization. From this geometry, hydrogen migration from the allylic carbon forms product **R5**. Transition state **TSR5** does not occur via elimination, but rather from an asynchronous 1,2-H shift temporarily forming an allylic carbocation followed by immediate formation of the alkene. The complete selectivity for the formation of a 1,3-diene is accounted for with our calculations: the 1,2-hydride shift initially generates a non-stationary carbocation β to gold(I) which is more stabilized when in resonance with the alkene than as a primary carbocation.

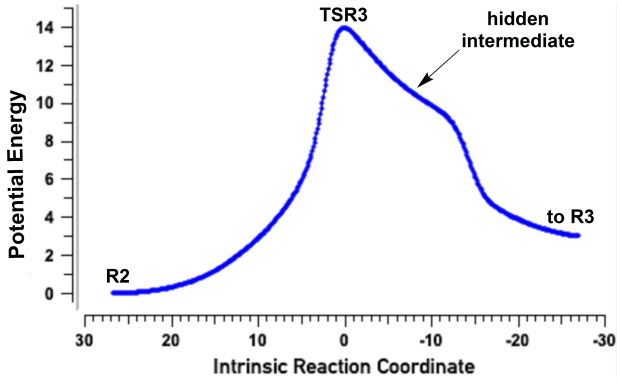

Figure 1. The IRC of **TSR3** reveals the presence of a hidden intermediate. Potential energy in kcal/mol.

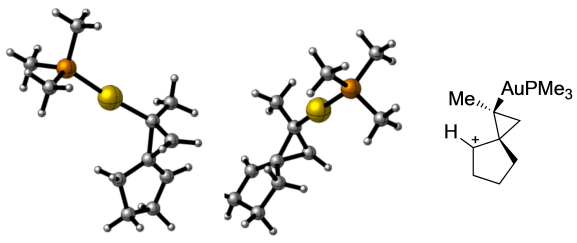

Figure 2. Structure of the key cyclopropylgold(I) hidden intermediate.

As **TSR3** is so close geometrically to the transition states for migration in exocyclic single cleavage rearrangements, and in the same family as the endocyclic migrations, the similarity in the reaction coordinate shines light on the process. We propose that the transition states in which a formal carbene migration takes place (**TS–SC$_{exo}$** and **TSR3**) are common to both single-cleavage and double-cleavage processes. This is supported by the fact that the cyclopropylgold(I) carbocation hidden intermediate appears in the barrierless relaxation of **TSR3** and the analogous transition state in the exocyclic single cleavage, belonging to the reaction coordinate of both processes. The structure of the product of migration would then be determined not by the migration itself, but by which bond of the cyclopropane breaks barrierlessly in the hidden intermediate.

Thus, cleavage of either of two cyclopropane bonds is barrierless and forms a different product: the cleavage of the bond α to gold(I) results in double cleavage rearrangement, whereas cleavage of the bond β to gold(I) results in single-cleavage rearrangement (Scheme 9, bonds marked in blue and red). Therefore, it is not the prior transition state but the non-stationary geometry that dictates the selectivity of the reaction in a barrierless process without intervening intermediates. The mechanistic relevance of the evolution of this geometry is analogous to that of other cases with hidden intermediates in concerted asynchronous processes.[19]

For the endocyclic single-cleavage rearrangement, the cyclopropyl gold carbocation constitutes a minimum and, therefore, different transition states for the *endo*-type single-cleavage and the unreported *endo*-type double-cleavage rearrangements are expected to exist and compete.[11] Due to the importance in determining what product is formed, the electronic properties of this cyclopropyl gold carbocation geometry are critical in fully understanding enyne skeletal rearrangements and related mechanisms in gold(I) catalysis.

This approach also explains the greater tendency for 1,6-enynes consisting of a terminally substituted alkyne and a terminally unsubstituted alkene to engage in double-cleavage rearrangements: the hidden intermediate evolves through formation of a gold(I)-stabilized carbocation –a gold(I) carbene– instead of the disfavored primary carbocation geometry that precedes the alkene as a non-stationary point in single-cleavage processes (Scheme 9).

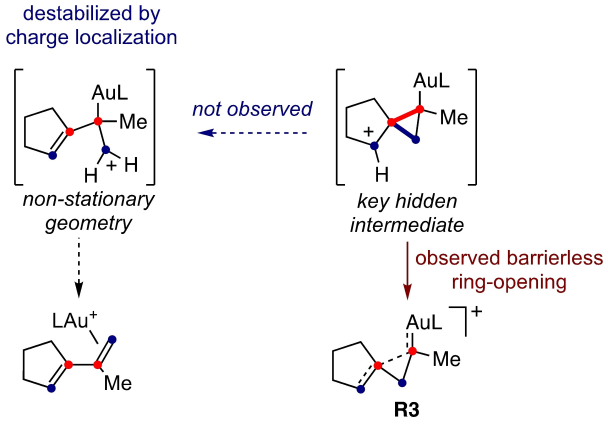

Scheme 9. The outcome of single- and double-cleavage rearrangements of 1,6-enynes depends on the evolution of a non-stationary hidden intermediate after the rate-determining step.

Both single-cleavage and double-cleavage reach the common key hidden intermediate and thus direct product formation is fully selective for one of the two pathways. Stepwise alternatives would be more likely to lead to mixtures of single- and double-cleavage products, as the transition states could compete, and it would be possible for them to be close in energy. The fact that the reaction outcome is not due to a competition between two transition states is consistent with what had been observed experimentally: substrates only undergo single-cleavage or double-cleavage skeletal rearrangements in gold(I)-catalyzed rearrangements but rarely both.

Conclusions

The intermediates present in gold(I)-catalyzed cyclizations of 1,5-enynes consist of cyclopropyl gold(I) carbenes and vinylgold(I) complexes with an endocyclic carbocation. Exocyclic carbocations without more significant stabilization are not minima on the potential energy surface, independently of whether the intermediate formed in *endo*-dig or *exo*-dig cyclizations, even for trisubstituted alkenes. As 1,6-enynes with trisubstituted alkenes can access the exocyclic carbocationic intermediates, the change in stability is likely related to ring strain and geometric proximity in a cyclopentenyl gold(I) carbocation. The cyclopropyl gold(I) carbene structures for 1,5-enynes were invariably lower in energy than the corresponding endocyclic carbocations, even with aryl substitution and for bicyclo[2.1.0]pentane systems. **Int4** geometries are particularly polarized **Int2** structures, and do not show significant differences in the NBO analysis as seen for fully open vinylcarbocations. They are best understood as a cyclopropyl gold(I) carbene system with a large contribution of the open form endocyclic carbocation resonance structure.

While 1,5-allenenes ultimately lead to the same bicyclic systems, non-classical carbocationic intermediates may also form. In all cases, these cyclize further to form the much more stable bicyclic structure. However, the intermediacy of open form six-membered ring endocyclic intermediates **5**, as proposed in the literature, is not supported by our calculations, as with 1,5-enynes.

Regarding the computational techniques employed, most functionals were found to be adequate by assessing the NBO charges of a particular intermediate, which generally correlate with the electronic description. In terms of determining the energy profile, our results indicate that, among those tested, B3LYP-D3 and M06-D3 are more accurate for gold(I)-catalyzed cyclizations at the level of theory employed in terms of their performance against the DLPNO-CCSD(T) benchmark.

A cyclopropyl gold(I) carbocation structure, which exists as a hidden intermediate in the exocyclic single- and double-cleavage skeletal rearrangements, defines the outcome of the reaction. The concerted asynchronous process of rate-limiting 1,3-migration followed by product-determining ring opening explains why only either the single-cleavage or double-cleavage products are found for a given substrate. We present the factors

that lead to substrate dependence, which are primarily electronic in nature. Additionally, we show that the final step in the formation of the double-cleavage product is a hydrogen migration instead of a deprotonation-protodemetallation sequence.

Supporting Information

The authors have cited additional references within the Supporting Information.[27–45] A set of the computational data underlying this study is available in the ioChem-BD repository and can be openly accessed at https://doi.org/10.19061/iochem-bd-1-289.

Acknowledgements

We thank the MCIN/AEI/10.13039/501100011033 (PID2022-136623NB–I00, PID2020-112825RB–I00, and CEX2019-000925-S), the European Research Council (Advanced Grant 835080), the AGAUR (2021 SGR 01256 and predoctoral fellowship to EG–P (2020FI_B 00403)), and CERCA Program/Generalitat de Catalunya for financial support.

Conflict of Interests

The authors declare no conflict of interest.

Data Availability Statement

The data that support the findings of this study are available in the supplementary material of this article.

Keywords: allenenes · cycloisomerization · DFT calculations · enynes · gold(I) catalysis

[1] a) A. Fürstner, L. Morency, *Angew. Chem. Int. Ed.* **2008**, *47*, 5030–5033; *Angew. Chem.* **2008**, *120*, 5108–5111; b) A. S. K. Hashmi, *Angew. Chem. Int. Ed.* **2008**, *47*, 6754–6756; *Angew. Chem.* **2008**, *120*, 6856–6858; c) G. Seidel, R. Mynott, A. Fürstner, *Angew. Chem. Int. Ed.* **2009**, *48*, 2510–2513; *Angew. Chem.* **2009**, *121*, 2548–2551; d) D. Benitez, N. D. Shapiro, E. Tkatchouk, Y. Wang, W. A. Goddard, F. D. Toste, *Nat. Chem.* **2009**, *1*, 482–486; e) A. M. Echavarren, *Nat. Chem.* **2009**, 431–433; f) Y. Wang, M. E. Muratore, A. M. Echavarren, *Chem. Eur. J.* **2015**, *21*, 7332–7339; g) R. J. Harris, R. A. Widenhoefer, *Chem. Soc. Rev.* **2016**, *45*, 4533–4551.

[2] a) C. Nieto-Oberhuber, S. López, M. P. Muñoz, D. J. Cárdenas, E. Buñuel, C. Nevado, A. M. Echavarren, *Angew. Chem. Int. Ed.* **2005**, *44*, 6146–6148; *Angew. Chem.* **2005**, *117*, 6302–6304; b) A. Fürstner, P. W. Davies, *Angew. Chem. Int. Ed.* **2007**, *46*, 3410–3449; *Angew. Chem.* **2007**, *119*, 3478–3519; c) E. Jiménez-Núñez, C. K. Claverie, C. Bour, D. J. Cárdenas, A. M. Echavarren, *Angew. Chem. Int. Ed.* **2008**, *47*, 7892–7895; *Angew. Chem.* **2008**, *120*, 8010–8013; d) P. Pérez-Galán, N. J. A. Martin, A. G. Campaña, D. J. Cárdenas, A. M. Echavarren, *Chem. Asian J.* **2011**, *6*, 482–486.

[3] a) G. Seidel, A. Fürstner, *Angew. Chem. Int. Ed.* **2014**, *53*, 4807–4811; *Angew. Chem.* **2014**, *126*, 4907–4911; b) M. W. Hussong, F. Rominger, P. Krämer, B. F. Straub, *Angew. Chem. Int. Ed.* **2014**, *53*, 9372–9375; *Angew. Chem.* **2014**, *126*, 9526–9529; c) R. J. Harris, R. A. Widenhoefer, *Angew. Chem. Int. Ed.* **2014**, *53*, 9369–9371; *Angew. Chem.* **2014**, *126*, 9523–9525; d) M. Joost, L. Estévez, S. Mallet-Ladeira, K. Miqueu, A. Amgoune, D. Bourissou, *Angew. Chem. Int. Ed.* **2014**, *53*, 14512–14516; *Angew. Chem.* **2014**, *126*, 14740–14744; e) J. Wang, X. Cao, S. Lv, C. Zhang, S. Xu, M. Shi, J. Zhang, *Nat. Commun.* **2017**, *8*, 14625–14635; f) A. Zeineddine, F. Rekhroukh, E. D. S. Carrizo, S. Mallet-Ladeira, K. Miqueu, A. Amgoune, D. Bourissou, *Angew. Chem. Int. Ed.* **2018**, *57*, 1306–1310; *Angew. Chem.* **2018**, *130*, 1320–1324.

[4] C. García-Morales, X.-L. Pei, J. M. Sarria Toro, A. M. Echavarren, *Angew. Chem. Int. Ed.* **2019**, *58*, 3957–3961; *Angew. Chem.* **2019**, *131*, 3997–4001.

[5] I. Escofet, H. Armengol-Relats, H. Bruss, M. Besora, A. M. Echavarren, *Chem. Eur. J.* **2020**, *26*, 15738–15745.

[6] C. Nieto-Oberhuber, P. Pérez-Galán, E. Herrero-Gómez, T. Lauterbach, C. Rodríguez, S. López, C. Bour, A. Rosellón, D. J. Cárdenas, A. M. Echavarren, *J. Am. Chem. Soc.* **2008**, *130*, 269–279.

[7] a) C. Obradors, A. M. Echavarren, *Acc. Chem. Res.* **2014**, *47*, 902–912; b) R. Dorel, A. M. Echavarren, *Chem. Rev.* **2015**, *115*, 9028–9072.

[8] a) L. Goerigk, S. Grimme, *Phys. Chem. Chem. Phys.* **2011**, *13*, 6670–6688; b) L. Goerigk, H. Kruse, S. Grimme, *ChemPhysChem.* **2011**, *12*, 3421–3433; c) F. O. Evers, F. Formalik, A. Olejniczak, M. Fischer, *Theor. Chem. Acc.* **2016**, *135*, 257; d) S. Dohm, A. Hansen, M. Steinmetz, S. Grimme, M. P. Checinski, *J. Chem. Theory Comput.* **2018**, *14*, 2596–2608; e) C. Riplinger, B. Sandhoefer, A. Hansen, F. Neese, *J. Chem. Phys.* **2013**, *139*, 134101; f) M. A. Iron, T. Janes, *J. Phys. Chem.* **2019**, *123*, 3761–3781.

[9] a) Atoms in Molecules. A Quantum Theory, R. F. W. Bader, Clarendon Press **1994**; b) R. F. W. Bader, *Chem. Eur. J.* **2006**, *12*, 7769–7772.

[10] a) Valency and Bonding: A Natural Bond Orbital Donor-Acceptor Perspective, C. R. Landis, F. W. Weinhold, Cambridge University Press **2005**; b) C. R. Landis, F. Weinhold, *J. Am. Chem. Soc.* **2006**, *128*, 7335–7345.

[11] E. García-Padilla, F. Maseras, A. M. Echavarren, *ACS Org. & Inorg. Au* **2023**, DOI: 10.1021/acsorginorgau.3c00028.

[12] a) M. Álvarez-Moreno, C. De Graaf, N. López, F. Maseras, J. M. Poblet, C. Bo, *J. Chem. Inf. Model.* **2015**, *55*, 95–103; https://iochem-bd.iciq.es/browse/review-collection/100/64662/f9bb726a831c07af6c34d67.

[13] a) A. D. Becke, *Phys. Rev. A.* **1988**, *38*, 3098–3100; b) J. P. Perdew, *Phys. Rev. B.* **1986**, *33*, 8822–8824.

[14] For further details on calculated bond distances and angles of optimized intermediates by DFT see the Supporting Information.

[15] M. R. Luzung, P. Mauleón, F. D. Toste, *J. Am. Chem. Soc.* **2007**, *129*, 12402–12403.

[16] a) N. Semleit, G. Haberhauer, *Org. Lett.* **2021**, *23*, 9635–9639; b) C. Chen, Y. Zou, X. Chen, X. Zhang, W. Rao, P. W. H. Chan, *Org. Lett.* **2016**, *18*, 4730–4733; c) A. Buzas, F. Gagosz, *J. Am. Chem. Soc.* **2006**, *128*, 12614–12615; d) X. Chen, Y. Zhou, J. Jin, K. Farshadfar, A. Ariafard, W. Rao, P. W. H. Chan, *Adv. Synth. Catal.* **2020**, *362*, 1084–1095.

[17] N. Marion, G. Lemière, A. Correa, C. Costabile, R. S. Ramón, X. Moreau, P. de Frémont, R. Dahmane, A. Hours, D. Lesage, J.-C. Tabet, J.-P. Goddard, V. Gandon, L. Cavallo, L. Fensterbank, M. Malacria, S. P. Nolan, *Chem. Eur. J.* **2009**, *15*, 3243–3260.

[18] a) E. Kraka, D. Cremer, *Acc. Chem. Res.* **2010**, *43*, 591–601; b) D. Roca-López, V. Polo, T. Tejero, P. Merino, *J. Org. Chem.* **2015**, *80*, 4076–4083.

[19] a) H. S. Rzepa, C. Wentrup, *J. Org. Chem.* **2013**, *78*, 7565–7574; b) G. Garay, J. Hurtado, M. Pedrón, L. García, E. Reyes, E. Sánchez-Díez, T. Tejero, L. Carrillo, P. Merino, J. L. Vicario, *Angew. Chem. Int. Ed.* **2023**, *62*, e202302416; c) R. Durán, C. Barrales-Martínez, R. A. Matute, *Phys. Chem. Chem. Phys.* **2023**, *25*, 6050–6059.

[20] S. Grimme, *WIREs Comput. Mol. Sci.* **2011**, *1*, 211–228.

[21] For further information on the benchmark of DFT functionals see the Supporting Information.

[22] a) C. Nieto-Oberhuber, M. P. Muñoz, S. López, E. Jiménez-Núñez, C. Nevado, E. Herrero-Gómez, M. Raducan, A. M. Echavarren, *Chem. Eur. J.* **2006**, *12*, 1677–1693; b) A. Escribano-Cuesta, P. Pérez-Galán, E. Herrero-Gómez, M. Sekine, A. A. C. Braga, F. Maseras, A. M. Echavarren, *Org. Biomol. Chem.* **2012**, *10*, 6105–6111.

[23] N. Cabello, E. Jiménez-Núñez, E. Buñuel, D. J. Cárdenas, A. M. Echavarren, *Eur. J. Org. Chem.* **2007**, 4217–4223.

[24] C. Nieto-Oberhuber, S. López, M. P. Muñoz, D. J. Cárdenas, E. Buñuel, C. Nevado, A. M. Echavarren, *Angew. Chem. Int. Ed.* **2005**, *44*, 6146–6148.

[25] E. Soriano, J. Marco-Contelles, *Acc. Chem. Res.* **2009**, *42*, 1026–1036.

[26] a) L.-G. Zhuo, J.-J. Zhang, Z.-X. Yu, *J. Org. Chem.* **2012**, *77*, 8527–8540; b) L.-G. Zhuo, J.-J. Zhang, Z.-X. Yu, *J. Org. Chem.* **2014**, *79*, 3809–3820.

[27] Gaussian 09, Revision B.1, Frisch, M. J. Trucks, G. W. Schlegel, H. B. Scuseria, G. E. Robb, M. A. Cheeseman, J. R. Scalmani, G. Barone, V. Mennucci, B. Petersson, G. A. Nakatsuji, H. Caricato, M. Li, X. Hratchian,

H. P. Izmaylov, A. F. Bloino, J. Zheng, G. Sonnenberg, J. L. Hada, M. Ehara, M. Toyota, K. Fukuda, R. Hasegawa, J. Ishida, M. Nakajima, T. Honda, Y. Kitao, O. Nakai, H. Vreven, T. Montgomery, J. A. Peralta Jr, J. E. Ogliaro, F. Bearpark, M. Heyd, J. J. Brothers, E. Kudin, K. N. Staroverov, V. N. Kobayashi, R. Normand, J. Raghavachari, K. Rendell, A. Burant, J. C. Iyengar, S. S. Tomasi, J. Cossi, M. Rega, N. Millam, J. M. Klene, M. Knox, J. E. Cross, J. B. Bakken, V. Adamo, C. Jaramillo, J. Gomperts, R. Stratmann, R. E. Yazyev, O. Austin, A. J. Cammi, R. Pomelli, C. Ochterski, J. W. Martin, R. L. Morokuma, K. Zakrzewski, V. G. Voth, G. A. Salvador, P. Dannenberg, J. J. Dapprich, S. Daniels, A. D. Farkas, Ö. Foresman, J. B. Ortiz, J. V. Cioslowski, J. Fox, D. J. Gaussian, Inc., Wallingford CT **2009**.

[28] a) A. D. Becke, *J. Chem. Phys.* **1993**, *98*, 5648–5652; b) C. Lee, W. Yang, R. G. Parr, *Phys. Rev. B.* **1988**, *37*, 785; c) P. J. Stephens, F. J. Devlin, C. F. Chabalowsky, M. J. Frisch, *J. Phys. Chem.* **1994**, *98*, 11623–11627.

[29] S. Grimme, J. Antony, S. Ehrlich, H. Krieg, *J. Chem. Phys.* **2010**, *132*, 154104.

[30] W. J. Hehre, R. Ditchfield, J. A. Pople, *J. Chem. Phys.* **1972**, *56*, 2257–2261.

[31] D. Andrae, U. Haussermann, M. Dolg, H. Stoll, H. Preuss, *Theor. Chim. Acta* **1990**, *77*, 123–141.

[32] M. T. Cancès, B. B. Mennucci, J. Tomasi, *J. Chem. Phys.* **1997**, *107*, 3032–3041.

[33] a) L. Goerigk, S. Grimme, *Phys. Chem. Chem. Phys.* **2011**, *13*, 6670–6688; b) L. Goerigk, H. Kruse, S. Grimme, *ChemPhysChem.* **2011**, *12*, 3421–3433; c) F. O. Evers, F. Formalik, A. Olejniczak, M. Fischer, *Theor. Chem. Acc.* **2016**, *135*, 257; d) S. Dohm, A. Hansen, M. Steinmetz, S. Grimme, M. P. Checinski, *J. Chem. Theory Comput.* **2018**, *14*, 2596–2608.

[34] A. D. Becke, *Phys. Rev. A.* **1988**, *38*, 3098–3100.

[35] S. Grimme, *J. Comput. Chem.* **2006**, *27*, 1787–179.

[36] J. Tao, J. P. Perdew, *Phys. Rev. Lett.* **2003**, *91*, 146401.

[37] J. P. Perdew, K. Burke, M. Ernzerhof, *Phys. Rev. Lett.* **1996**, *77*, 3865–3868.

[38] A. D. Becke, *J. Chem. Phys.* **1993**, *98*, 5648–5652.

[39] A. D. Boese, J. M. Martin, *J. Chem. Phys.* **2004**, *121*, 3405–3416.

[40] Y. Zhao, D. G. Truhlar, *J. Chem. Phys.* **2006**, *125(104101)*, 1–18.

[41] C. Adamo, *J. Chem. Phys.* **1999**, *110*, 6158–6170.

[42] C. Riplinger, B. Sandhoefer, A. Hansen, F. Neese, *J. Chem. Phys.* **2013**, *139*, 134101.

[43] F. Neese, *WIREs Comput. Mol. Sci.* **2018**, *8*, e1327.

[44] a) Valency and Bonding: A Natural Bond Orbital Donor-Acceptor Perspective, C. R. Landis, F. W. Weinhold, Cambridge University Press **2005**; b) C. R. Landis, F. Weinhold, *J. Am. Chem. Soc.* **2006**, *128*, 7335–7345.

[45] M. Álvarez-Moreno, C. De Graaf, N. López, F. Maseras, J. M. Poblet, C. Bo, *J. Chem. Inf. Model.* **2015**, *55*, 95–103.

Manuscript received: September 5, 2023
Revised manuscript received: November 3, 2023
Accepted manuscript online: November 21, 2023
Version of record online: ■■, ■■

RESEARCH ARTICLE

The mechanism of the gold(I)-catalyzed cyclization of enynes and allenenes was clarified through a combination of calculations using B3LYP-D3, M06-D3 and DLPNO-CCSD(T) computational methods.

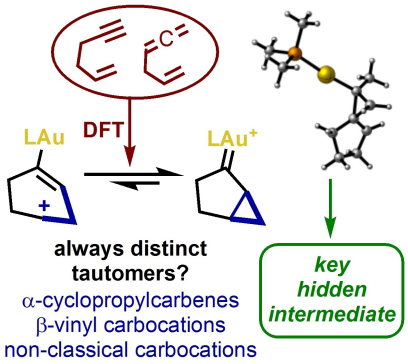

*E. García-Padilla, Dr. I. Escofet, Prof. F. Maseras, Prof. A. M. Echavarren**